The effects of proton induced radiation damage on compound semiconductor X-ray detectors

Alan Owens[1*], L. Alha[2], H. Andersson[3], M. Bavdaz[1], G. Brammertz[1], K. Helariutta[4], A. Peacock[1], V. Lämsä[3], S. Nenonen[3]

[1]Science Payload and Advanced Concepts Office, SCI-A, ESA/ESTEC, Postbus 299, 2200AG, Noordwijk, The Netherlands
[2]Helsinki Observatory, PO Box 14, FIN-00014, University of Helsinki, Finland
[3]Metorex International Oy, PO Box 85, FIN-02630, Espoo, Finland
[4]Laboratory of Radiochemistry, Department of Chemistry, PO box 55, Fin-00014, University of Helsinki, Finland

ABSTRACT

We report the results of a series of experiments designed to assess the relative radiation hardness of a range of compound semiconductor X-ray detectors. The specific compounds tested were GaAs, InP, CdZnTe, HgI_2 and TlBr, along with an elemental Si device. To allow meaningful comparisons, all devices were of a similar size and, with the exception of the InP detector, had sub-keV energy resolution at 5.9 keV. The irradiations were carried out using the University of Helsinki's Cyclone 10/5 10 MeV proton cyclotron. Each detector was given six consecutive exposures - the integral fluences being; 2.66×10^9 p cm^{-2}, 7.98×10^9 p cm^{-2}, 2.65×10^{10} p cm^{-2}, 7.97×10^{10} p cm^{-2}, 1.59×10^{11} p cm^{-2}, and 2.65×10^{11} p cm^{-2}, respectively. In Si, these correspond to absorbed radiation doses of 2, 6, 20, 60, 120 and 200 krads. During the exposures, the detectors were kept unbiased and at room temperature. After each irradiation, the effects of the exposure were assessed, both at room temperature and at a reduced temperature using ^{55}Fe, ^{109}Cd and ^{241}Am radioactive sources. It was found that with the exception of the HgI_2 and TlBr detectors all materials showed varying degrees of damage effects.

Keywords: Compound semiconductors, radiation damage, X-rays detectors; PACS: 29.30.KV, 29.40.Wk, 81.05.Dz, 81.05.Ea, 81.40.Wx

1. INTRODUCTION

Compound semiconductor X-ray detectors have evolved sufficiently to become viable candidates to be flown on future planetary and astrophysics missions. Compared to the elemental semiconductors Ge and Si, wide-gap compounds drawn from elements in groups II to VI of the periodic table are particularly interesting, especially from an operational and radiation tolerance point of view. For example, their larger bandgap energies offer the possibility of room temperature operation; thus alleviating the need for expensive and complicated cryogenic systems. Increasing the bandgap also increases the energy of defect formation making compound semiconductors intrinsically radiation hard. Additionally, because of their higher effective *Z's* and therefore X-ray stopping powers, detectors can be made thinner to maintain a given efficiency, with resulting reductions in mass, power, size and radiation damage (which is a bulk effect). Lastly, because oxide interfaces

*aowens@rssd.esa.int; phone 31-71-565-5326; fax 31-71-565-4690; http://astro.esa.int/ST-general/index.html

CERN LIBRARIES, GENEVA

CM-P00050909

are not used in compound semiconductor devices, they do not suffer from ionization radiation damage or from the space charge effects observed in Si detectors during large solar flares [1]. Although it is claimed that some compound semiconductor materials are extremely radiation hard, withstanding proton fluences as high as $10^{12}cm^{-2}$ [2], the tolerance of a large number of compounds to space radiation effects has yet to be demonstrated. In the case of the solar X-ray monitors, the requirement to observe the Sun directly (except for a thin Be window) mandates radiation tolerances to doses as high as a Mrad. In order to evaluate the robustness of compound semiconductors for space flight, we have irradiated a set of compound semiconductor detectors with 10 MeV protons up to a fluence of ~5 x 10^{11} protons cm^{-2}.

1.1 Radiation damage effects

Ionizing radiation damages semiconductor detectors through displacement, transient ionization and long term ionization effects. Ionization effects are generally only important for insulators (such as metal oxide interfaces) and result in an increase in dark current and subsequently noise. In Si, doses of up to 100 krad can be tolerated to some extent, with only a change in operating conditions. Displacement effects, on the other hand, result in permanent damage to the lattice structure. In essence, particle collisions with the semiconductor atoms introduce defects in the lattice, which act as carrier generation and trapping centers for non-equilibrium charge carriers. In detectors, they cause changes of the internal electric field, due to the modified doping concentration, an increase in leakage currents, changes in capacitance and resistivity, and if the trappings times are longer than the amplifier time constants, charge collection losses. For moderate damage, this is most easily identified and characterized by measuring the degradation in a detectors energy resolution function.

For space applications, the dominant source of damage arises from high energy protons, largely due to the large fluxes and interaction cross sections. Deuterons and α-particles can be neglected because of their relatively low fluences. Likewise, damage due to trapped electrons may be ignored because of their relatively soft spectra. The effects of photons can also be neglected, as the ambient flux of photons at MeV energies is many orders of magnitudes less than that of protons. Because damage is a highly non-linear function of particle energy, we have opted for direct measurement rather than a calculational approach. A description of the experiment and its results is given below.

2. EXPERIMENTAL

The irradiations were carried out on a range of detectors at the Department of Radiochemistry of the University of Helsinki, Finland. Protons were generated using a Cyclone 10/5 cyclotron system manufactured by Ion Beam Applications of Louvain-la-Neuve, Belgium. The machine is illustrated in fig.1 and is capable of accelerating H^- ions to 10 MeV and D^- ions to 5 MeV. Negative ions are produced in an external "multicusp" ion source and axially injected into the cyclotron. A high voltage alternating electric field is applied between the Dees, accelerating the ions, which are then confined to circulate within the Dees by a fixed magnetic field. At the extraction radius, the negative particles are stripped of their electrons by passing through a very thin carbon foil and the resulting positively charged ions (H^+ or D^+) are bent outwards to the target ports by the magnetic field. Up to 80 μA of proton beam intensity can be extracted at the exit ports. Although most targets are irradiated directly at the ports, an external UHV beam pipe is used for the irradiation of solid targets. A pair of quadrupoles is used to focus the beam and define its profile at the target.

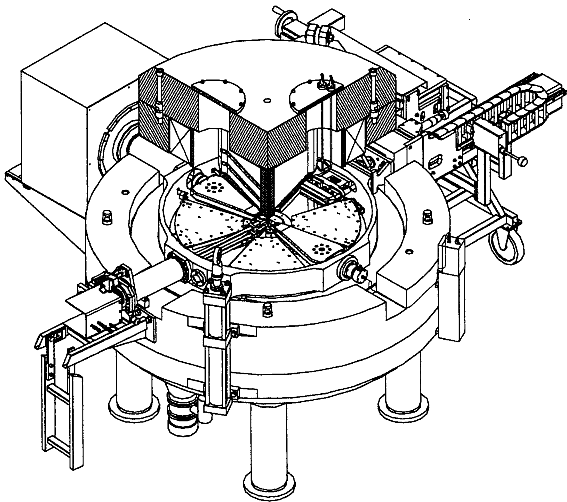

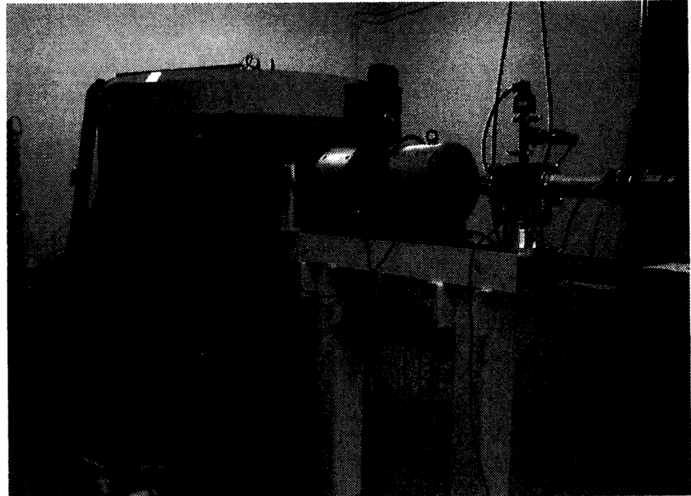

Fig. 1. Left: A cross-sectional view of the Helsinki IBA Cyclone 10/5 cyclotron shown right. This machine can deliver a 10 MeV proton beam at a maximum current of 80 μA. The detectors were mounted at the end of the beam pipe depicted in the right figure.

Irradiations were carried out on a range of detectors - 2 GaAs diodes, a Si diode, a TlBr detector, a CdZnTe detector, an HgI_2 detector and an InP detector. The detectors are packaged in aluminium vacuum housings and viewed through thin (25μm) Be windows. They are mounted on two stage Peltier coolers capable of cooling both the sensors and (shielded) front-end components to -30°C. The rest of the analog chain consists of an externally mounted resistive feedback or transistor reset preamplifier – the type depending on the level of the leakage current. All these devices were the end products of our compound semi-conductor research program [3] and had excellent resolutions for their type, thus ensuring that the comparison of radiation tolerance is reasonably representative. A pre-irradiation compilation of detector parameters is given in Table 1.

Table 1. The detectors used in the present studies. The energy resolution measurements were carried out under uniform illumination using ^{55}Fe, ^{109}Cd and ^{241}Am radioactive sources, prior to the irradiations. For completeness, we also list the resolutions at room temperature (RT) were possible, since there are many applications in which resolving power is not a primary requirement, *e.g.*, dosimetry.

Material	Detector size Area × thickness	ΔE @ 5.9 keV (eV)	ΔE @ 22.1keV (eV)	ΔE @ 59.5keV (eV)
Si	0.8 mm^2, 500 μm	245 @ -15°C	400	524
GaAs1	0.8 mm^2, 40 μm	450 @ -22°C 572 @ RT	600 570	670 780
GaAs2	0.8 mm^2, 40 μm	683 @ -30°C 1159 @ RT	730 1177	777 1192
InP	3.142 mm^2, 180 μm	2480 @ -60°C	6100	9200
CdZnTe	3.142 mm^2, 2.5 mm	450 @ -30°C 1508 @ RT	640	970 2900
HgI_2	7 mm^2, 500 μm	438 @ -19°C 618 @ RT	1540 1340	1540 2710
TlBr	3.142 mm^2, 800 μm	974 @ -30°C	1410	3400

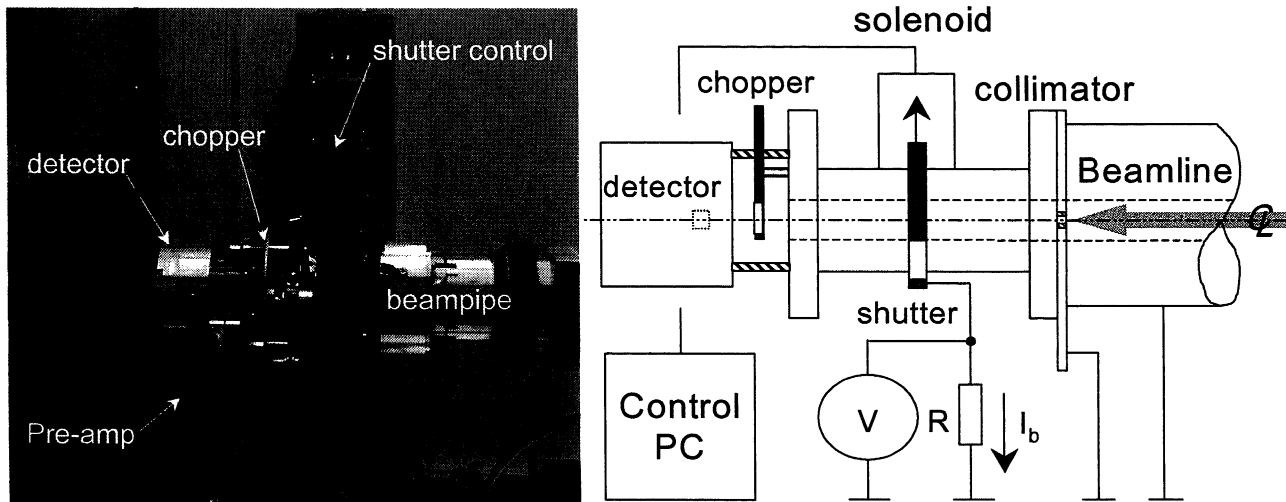

Fig. 2. Left: the beamline setup. Right: a functional view of the irradiation set-up. The proton flux at the detector is controlled by a shutter and chopper. The chopper is used to reduce the flux incident on the detector and the shutter to control the exposure. The typical irradiation fluence at the detector was $\sim 4 \times 10^8$ p cm^{-2} s^{-1} and the beam size 1.8 cm^2.

3. IRRADIATIONS

The detectors were coupled to the end of the beamline as shown in fig. 2. The proton beam current is measured by a beam shutter that is electrically insulated from the beam line. The shutter is made from a 3 mm aluminium plate and is operated by a PC that can open and close it with a 50 ms accuracy. Because of stability issues when operating at small beam currents, a relatively large beam current is input on the shutter which is subsequently reduced further downstream using a beam chopper with one 2° sector. Thus, the beam current was decreased to 1/180 of its original intensity, allowing longer exposure times to be used with a subsequent decrease in local heating of the samples as well the errors induced in the exposures due to the finite shutter response. The exposure procedure is as follows. The shutter (see fig. 2 - right) starts in the closed position and the current induced by the impinging beam measured with an electrometer. The exposure time is then computed from the beam current and input to the shutter control software, which operates the shutter *via* the serial port of the computer. During exposures the cyclotron settings were kept constant. The ion source current was 115 mA, the acceleration voltage (Dee voltage) 31.9 kV and the main coil current 143 A. The ion source current was manually set to 1 in an arbitrary scale of 1000, corresponding to approxamtely 10 nA beam current, or alternatively, an incident flux at the detectors of 4×10^8 p cm^{-2}s^{-1}. Finally, the diameter of the beam at the detectors was set to 15 mm by a pair of quadrupoles – this being sufficient to uniformly illuminate the surface area of the largest detector.

2.1 Dose philosophy

Ioinization/ depth profiles were generated for each detector material using TRIM. From the ionisation curves, it was clear that 10 MeV protons would not pass all the way through the thicker detectors. In fact, dose depth curves show that detector materials should have a thickness of no more than ~ 200 microns for an unbiased inter-comparative radiation damage test to be carried out. Normally, one would attempt to give the same dose to each detector after correcting for detector thickness. However, given the wide range of thicknesses of the

test detectors (40 microns to 2500 microns), it would not be feasible to give all detectors the same dose, since in the thicker detectors the radiation damage will be entirely confined to a narrow layer below the irradiated surface, whereas in a thin detector it will be uniformly distributed all the way through. Additionally, the ionization energy losses in thick detectors will be disproportionate and very non-uniform with depth, since most of it is due to particles at the end of their range. Therefore we carried out the following. The dose equivalent number of protons was calculated for the Si detector. All detectors were then given the same number of particles, with the exception that the second GaAs detector (GaAs2) was tested with the same dose equivalent. This corresponds to about twice the number of protons per irradiation than the other detectors. Thus, one GaAs diode is exposed to the same number of particles and the other the same dose in krads. This has an advantage for space applications in than it is possible to compare materials on a straight proton for proton basis (which is encountered in space) as well as compare materials to different radiation environments based on an interpretation of NIEL curves.

4. MEASUREMENTS

Each detector was given six, logarithmically spaced, consecutive exposures - the integral fluences after each being; 2.66×10^9 p cm^{-2}, 7.98×10^9 p cm^{-2}, 2.65×10^{10} p cm^{-2}, 7.97×10^{10} p cm^{-2}, 1.59×10^{11} p cm^{-2}, and 2.65×10^{11} p cm^{-2}, respectively. In Si, these correspond to absorbed radiation doses of 2, 6, 20, 60, 120 and 200 krads. The corresponding fluences for GaAs2 were: 4.64×10^9 p cm^{-2}, 1.39×10^{10} p cm^{-2}, 4.63×10^{10} p cm^{-2}, 1.39×10^{11} p cm^{-2}, 2.78×10^{11} p cm^{-2} and 4.64×10^{11} p cm^{-2}.The irradiation history for each detector is listed in Table 2. We also list the absorbed dose in each detector material. During exposures, which lasted typically 20 to 200 secs, the detectors were kept unbiased and at room temperature. After each irradiation, the effects of the exposure were assessed, both at room temperature and at a reduced temperature (typically –20°C) using ^{55}Fe, ^{109}Cd and ^{241}Am radioactive sources. These measurements were carried out between 3 and 24 hours later, depending on the level of the leakage current and detector stability. Indeed, after some of the larger exposures (> ~10^{11} p cm^{-2}), measurements could not be carried out for weeks on the Si and CdZnTe detectors. Other than cycling between room and operating temperature, the detectors were not annealed.

Table 2. Irradiation history of the devices. For each irradiation, we list the number of incident protons as well as the absorbed dose in krads. GaAs2 was given the same Si dose equivalent, which corresponds to about twice the Si fluence.

Compound	Irradiation history	Accumulated dose p cm^{-2}				
	2.66×10^9	7.98×10^9	2.65×10^{10}	7.97×10^{10}	1.59×10^{11}	2.65×10^{11}
	Total dose krads					
Si	2.0	6.0	20.0	60.0	120.0	not irradiated
InP	1.31	3.97	13.1	39.3	78.6	130.7
GaAs1	1.15	3.44	11.44	34.3	68.7	114.2
HgI_2	1.05	3.16	10.5	31.6	63.1	105.0
TlBr	0.6	1.8	6.0	18.0	36.0	60.2
CdZnTe	0.31	0.85	3.2	9.3	18.6	31.0
Total dose p cm^{-2}	4.64×10^9	1.39×10^{10}	4.63×10^{10}	1.39×10^{11}	2.78×10^{11}	4.64×10^{11}
GaAs2	2.0	6.0	20.0	60.0	120.0	200.0

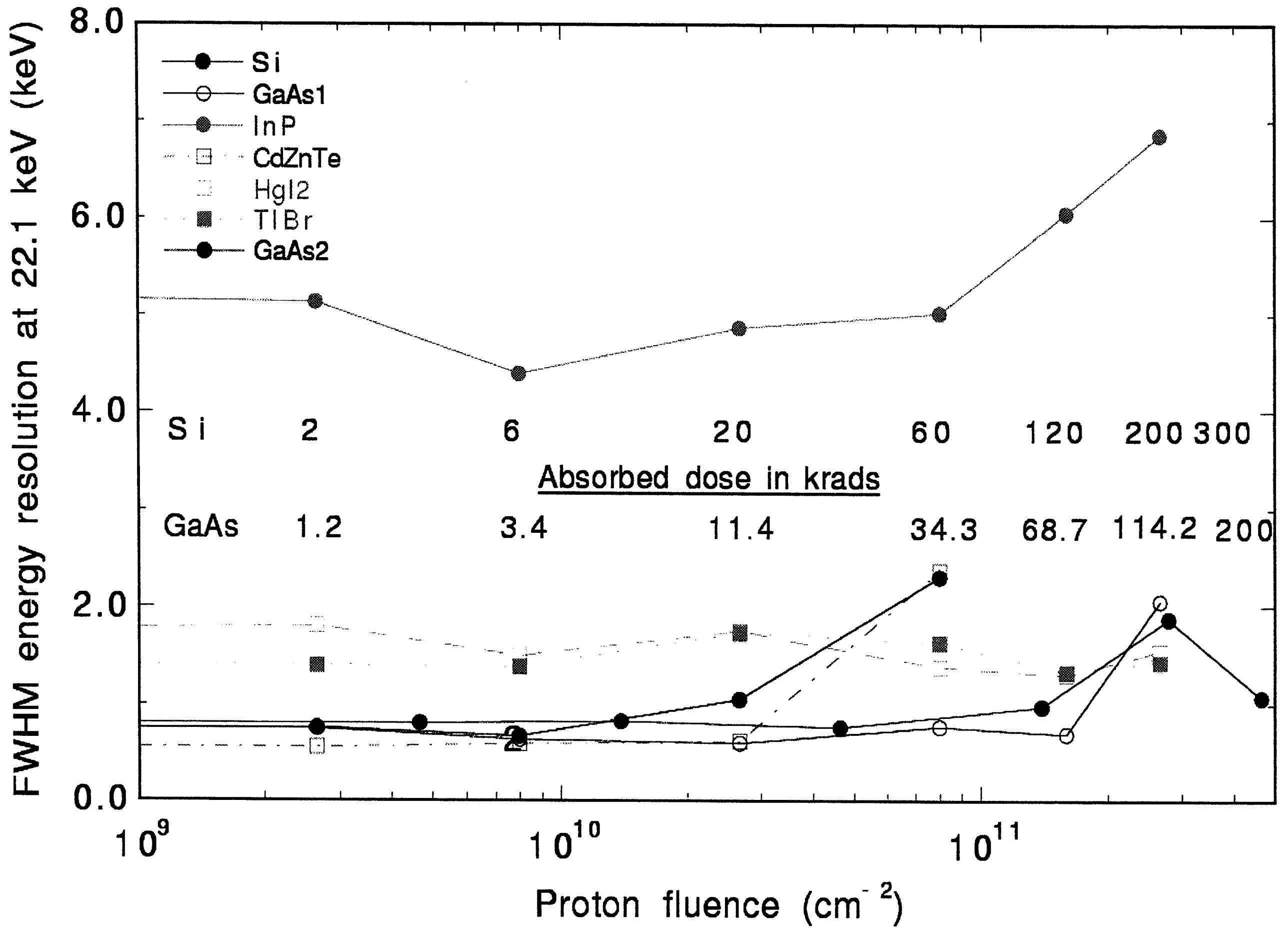

Fig. 3. The measured fwhm energy resolutions at 22 keV as a function of proton fluence. The absorbed doses (krads) in Si (blue) and GaAs (black) are also indicated. Note the resolutions were taken at the optimum shaping time.

6. RESULTS

In fig. 3, we plot the measured fwhm energy resolutions at 22 keV as a function of proton fluence. The absorbed doses (krads) in Si and GaAs are also indicated. The immediate observable effect of damage is an increase in leakage current, resulting in shorter amplifier shaping times to optimize energy resolution. It is these values that are plotted in fig. 3. Note: the detector biases were kept at the same values throughout this study. Simply stated, Si began degrading immediately at the first irradiation of 2.7×10^9 cm^{-2}, followed by CdZnTe at a fluence of 8.0×10^{10} cm^{-2}, followed by GaAs at a fluence of 1.6×10^{11} cm^{-2}. The other detectors maintained their resolutions within statistics. The data are tabulated in Table 3 in which we list the fractional energy resolutions at 22 keV (*i.e.,* those measured at a particular fluence divided by their pre-irradiation values) for each irradiation – thus damaged detectors should have a ratio > 1. The last column gives the average value by which we have ranked the data. Note, for simplicity we have offset the values of GaAs2 by one column, since this detector was given approximately twice the fluence per irradiation than the others. Below, we describe in more detail the individual responses of each detector material.

Table 3. Summary of radiation effects in compound semiconductors. What is listed are the ratios of the measured energy resolutions after each exposure to their initial pre-irradiation values. The last column gives the average value. The data are ranked by this value. The dashed line delineates the boundary of measurable radiation damage.

Dose $p\ cm^{-2}$	2.7×10^9	8.0×10^9	2.7×10^{10}	8.0×10^{10}	1.6×10^{11}	2.7×10^{11}	4.6×10^{11}	Average factor
InP	0.8	0.7	0.8	0.8	1.0	1.1		0.9
TlBr	1.0	1.0	1.2	1.1	0.9	1.0		1.0
HgI_2	1.3	1.3	1.1	1.0	1.0	1.0		1.1
GaAs2		1.1	1.1	1.0	1.3	2.5	1.4	1.4
GaAs1	1.2	1.0	0.9	1.2	1.1	3.3		1.5
CdZnTe	0.9	0.9	0.9	3.6	2.9	Unmeasurable		1.8
Si	1.9	1.7	2.6	Unmeasurable	2.6	Unmeasurable		2.1

Si: Silicon exhibited a factor of ~ two degradation in energy resolution after the first irradiation of 2×10^9 p cm^{-2}. After each subsequent exposure, it took the detector an increasingly longer time to recover – much longer than for the other detectors. Furthermore, while the charge pulses looked nominal on an oscilloscope, the baseline signal was found to vary erratically, resembling telegraph noise.

CdZnTe: Cadmium zinc telluride started showing effects after 2×10^{10} p cm^{-2} becoming virtually unusable after 8×10^{10} p cm^{-2}. After 2×10^{10} p cm^{-2} the recorded spectra showed double peaked structure – the peaks becoming increasing separated with dose.

GaAs: Both GaAs detectors showed little variation up to a fluence of 2×10^{10} p cm^{-2}, other than a progressive decrease in shaping time. The devices then degraded by a factor of ~ two after a total dose of 3×10^{11} p cm^{-2}.

TlBr: Thalium bromide was found to withstand radiation proton fluences up to 3×10^{11} cm^{-2}, but after 8×10^{10} protons cm^{-2} it was observed that polarization effects had increased significantly. These manifest themselves as gain shifts and spectral broadening that is proportional to the total energy deposition per unit time. In pre-irradiation measurements, it was found that these effects only became evident for energies above 50 keV and count rates above 200 s^{-1}. However, after an exposure of 8×10^{10} protons cm^{-2}, polarization effects were now evident at energies as low as 15 keV at 200 counts s^{-1}.

HgI_2: Mercuric Iodide showed no significant variation or increase in polarization effects (which are commonly observed in undamaged HgI_2 detectors) due to the irradiations.

InP: Likewise, indium phosphide also showed no change across the entire dose range. However, it could be argued that because the resolution was so poor to begin with (6.1 keV FWHM at 22 keV), one might not expect to see a significant change. Since its properties are very similar to GaAs, we might reasonably expect it to behave in a similar fashion if its energy resolution was comparable.

After the sixth and final irradiation the detectors were left for one and a half years before re-testing whereupon some recovery of the performance properties was observed, presumably due to annealing at room temperature. The Si detector in particular showed better stability and an improved energy resolution of 1 keV FWHM at 22 keV. The second GaAs (GaAs2) detector also showed a factor two improvement in energy

resolution after the same period (from 1.9 keV FWHM to 1.1 keV FWHM), despite the fact that it received the highest radiation dose of of 5×10^{11} p cm^{-2}. The other detector materials did not show a room temperature annealing effect and still behave in the same way as one and a half years earlier. For those detectors that displayed damage effects, the sensors were further annealed by raising their temperatures to 80°C for several weeks. All detectors were found to recover to some extent. Unfortunately, the Si detector still awaits testing, due to a failure of its Peltier element. The second GaAs detector (GaAs2) showed the largest recovery. After spending two weeks at a temperature of 80°C, the energy resolution decreased to 900 eV at 22 keV, which is within ~10% of its pre-irradiation resolution. The residual broadening remaining in the spectra arises from a low energy tail, probably caused by hole trapping. Annealing the detector for another two weeks at 80 °C did not improve the resolution further. Continued annealing of the CdZnTe detector has not significantly improved its performance. After the final irradiation, the detector constantly lost stability within 20 minutes after being biased. Whereas during the first minute the count rate is high and energy resolution is of the order of 1 keV, the count rate and gain of the detector then gradually decreased to virtually zero after about 20 to 30 minutes. After four weeks of annealing at 80 °C the detector is still unstable, however it now takes approximately 24 hours for its response to decrease to zero. Continued annealing will be carried out over the coming months to see whether further improvements can be made.

Table 4. The factors affecting the calculated absorbed dose. For inter-comparison we list the absorbed doses for a proton irradiation of 2.66×10^{9} p cm s^{-1}. The data are ranked by the product of the average nuclear charge and atomic density. The last column gives the "Tolerance" index for each of the materials (see text), which does not track the absorbed dose.

Compound	Bandgap eV	Atomic density cm^{-3}	Av. Nucl. Charge	Product cm^{-3}	Absorbed dose krads	Tolerance
CdZnTe	1.57	1.57×10^{22}	109.5 17	17.15×10^{23}	0.23	5
TlBr	2.68	1.60×10^{22}	53.2	8.52×10^{23}	0.60	3‡
HgI_2	2.13	0.84×10^{22}	92.1	7.81×10^{23}	1.05	1
GaAs	1.43	2.21×10^{22}	32.0	7.08×10^{23}	1.15	2
InP	1.35	1.98×10^{22}	27.1	5.38×10^{23}	1.31	4†
Si	1.12	4.97×10^{22}	5.29	2.63×10^{23}	2.00	6

‡moved from 2nd position to 3rd because of much increased polarization effects.
†moved to 4th because of it very poor initial energy resolution and its electronic and structural similarity to GaAs.

7. DISCUSSION AND CONCLUSIONS

Coulomb processes dominate the absorbed radiation dose in solid-state matter, which means that the stopping power for charged particles is dependent on *a)* the average atomic mass, *b)* the nuclear charge of the target nuclei and to a lesser extent *c*) the atomic density of the target material. In fact, the absorbed dose decreases with increasing density of the nuclear charge and decreases with the average atomic density of the medium. This can be seen in Table 4, where for example, we note that the absorbed dose for CdZnTe is low because it has a high average nuclear charge density combined with a reasonably high atomic density. This can be compared to other compounds which have higher absorbed doses for the same particle fluences, for example, HgI_2 due to its relatively a quite low atomic density and InP due to its low average nuclear charge density. However, while these parameters can be used as a guide, they do not uniquely identify which compounds are the most susceptible. For example, while experimentally, HgI_2 is the most radiation-hard material tested, CdZnTe is the worst (apart from Si) yet the latter has a much lower absorbed dose. Nor does hardness

correlate well with band-gap energy. Finally, the last column of Table 4 is labelled "Tolerance" and is ranked from 1 to 6 with 1 being the most tolerant. It is based on the last column of Table 3, with two subjective modifications. The first is that TlBr was moved from 2nd position to 3rd position because of the much increased polarization effects and secondly, that InP should be moved from 1st to 4th position because of its extremely poor initial energy resolution and its electronic and structural similarity to GaAs.

In conclusion, for doses up 2.65×10^{11} protons cm^{-2}, HgI_2 is the most radiation hard material, followed by TlBr. However, the latter begins to suffer from severe polarization effects at 1/50 of this dose. The least radiation hard materials are Si followed by CdZnTe. At present annealing is still being carried out. However at this juncture, we can state that only GaAs has responded significantly, returning to within 10% of its pre-irradiation value.

AKNOWLEDGEMENTS

We wish to thank IBA, Belgium for providing the illustrations of the Cyclone 10/5 and Jarkko Laukkanen for the dose calculations. Part of this work was supported by the IHP-Contract, HPRI-CT-1999-00040 of the European Commission.

REFERENCES

1. J. Trombka, *et al.*, Meteoritics and Planetary Science, **36** (2001) 1605.
2. F. Becchetti *et al.,* IEEE Trans. Nucl. Sci., **23** (1976) 468.
3. A. Owens, A. Peacock, M. Bavdaz, Proc. of the SPIE, **4851** (2003) 1059.